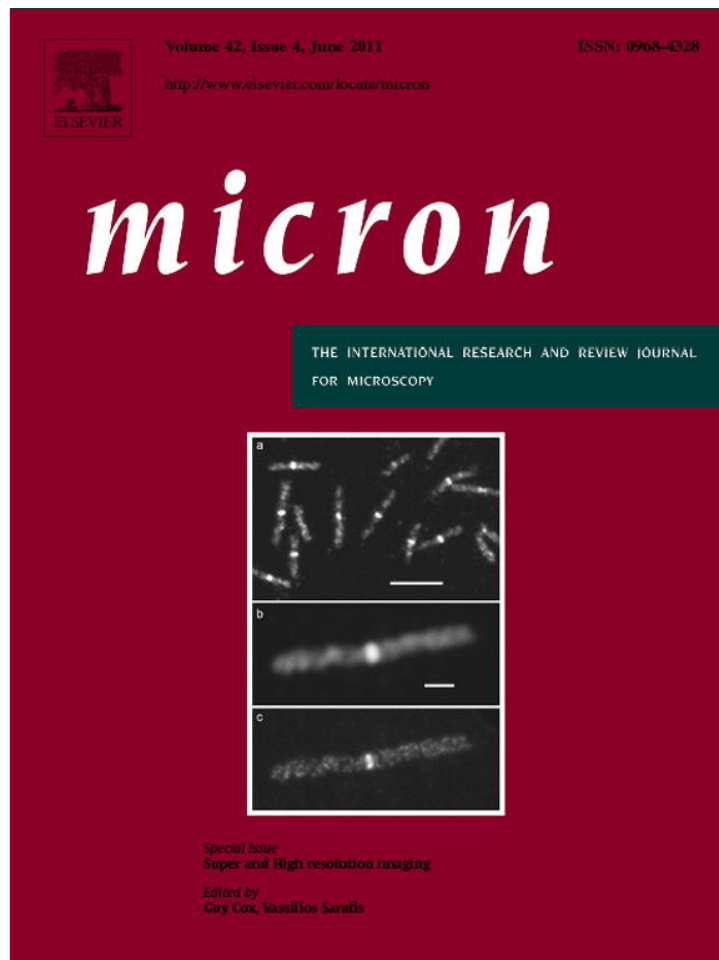


Provided for non-commercial research and education use.
Not for reproduction, distribution or commercial use.



This article appeared in a journal published by Elsevier. The attached copy is furnished to the author for internal non-commercial research and education use, including for instruction at the authors institution and sharing with colleagues.

Other uses, including reproduction and distribution, or selling or licensing copies, or posting to personal, institutional or third party websites are prohibited.

In most cases authors are permitted to post their version of the article (e.g. in Word or Tex form) to their personal website or institutional repository. Authors requiring further information regarding Elsevier's archiving and manuscript policies are encouraged to visit:

<http://www.elsevier.com/copyright>



Contents lists available at ScienceDirect

Micron

journal homepage: www.elsevier.com/locate/micron

Imaging label-free intracellular structures by localisation microscopy

Rainer Kaufmann^a, Patrick Müller^b, Michael Hausmann^b, Christoph Cremer^{a,c,d,*}

^a Applied Optics and Information Processing, Kirchhoff-Institute for Physics, University Heidelberg, Im Neuenheimer Feld 227, D-69120 Heidelberg, Germany

^b Peptide-Chips and Nucleotide FISH, Kirchhoff-Institute for Physics, University Heidelberg, Im Neuenheimer Feld 227, D-69120 Heidelberg, Germany

^c Institute for Pharmacy and Molecular Biotechnology, University Heidelberg, Im Neuenheimer Feld 364, D-69120 Heidelberg, Germany

^d Institute for Molecular Biophysics, The Jackson Laboratory, 600 Main Street, Bar Harbor, ME 04609, USA

ARTICLE INFO

Article history:

Received 15 January 2010

Received in revised form 8 March 2010

Accepted 9 March 2010

Keywords:

Sub-diffraction limit microscopy

Localisation microscopy

Spectral Precision Distance Microscopy

(SPDM)

Fluorescence

ABSTRACT

Localisation microscopy methods allow to realize a light optical resolution far beyond the Abbe–Rayleigh limit of about 200 nm laterally and 600 nm axially. So far, this progress was achieved using labelling with appropriate fluorochromes and fluorescent proteins. Here, we describe for the first time that optical resolution of cellular structures in the $\lambda/10$ range (~ 50 nm) can be achieved even in label-free cells. This was obtained using Spectral Precision Distance/Position Determination Microscopy (SPDM), a method based on the general principles of localisation microscopy. Besides a substantial resolution improvement of autofluorescent structures, SPDM revealed cellular objects which are not detectable under conventional fluorescence imaging conditions.

© 2010 Elsevier Ltd. All rights reserved.

1. Introduction

In the last decades, light microscopy has re-emerged as one of the fundamental methods in biomedical sciences and cellular biophysics. Typically, cellular structures are analysed by labelling with specific fluorophores which can be imaged using a fluorescence microscopy setup. Widely used methods for specific labelling are fluorochrome conjugated antibodies, or co-expressed fluorescent proteins (e.g. GFP).

A serious impediment to exploit the full potential of light microscopy to study cellular structures has been the conventional optical resolution of about 200 nm laterally and 600 nm axially, the Abbe–Rayleigh limit (Abbe, 1873; Rayleigh, 1896). This limit is still valid for all approaches using the basic conditions stated by Abbe and Rayleigh.

Novel approaches in light microscopy enabled effective optical resolutions down to about 20 nm. One of these methods is localisation microscopy. It is based on the fundamental concept of using fluorophores that can be switched between two different spectral states to achieve a temporal isolation and thus a spatial separation of single signals. This allows to determine the positions of the detected fluorophores even if they are close together (<200 nm). All acquired positions of fluorescent molecules can be merged into

one image, in which the effective resolution is determined by the localisation accuracy and the density of the detected signals. Early localisation microscopy approaches (SPDM) describe a localisation precision of 50 nm and less for point like fluorescent objects (Esa et al., 2000; Rauch et al., 2008). Using appropriate dye molecules other techniques (PALM (Betzig et al., 2006), FPALM (Hess et al., 2006), STORM (Rust et al., 2006)) improved the localisation accuracy down to 20 nm and allowed visualisation of large cellular structures. Here, special fluorophores are required, which can be switched between two spectral states using an appropriate additional laser source.

Recently, a novel method of localisation microscopy using conventional fluorophores (e.g. fluorescent proteins or Alexa dyes) was developed (SPDM (Lemmer et al., 2008)). The molecules are switched to a “dark” state by a light induced reversible photo bleaching (Hendrix et al., 2008; Patterson and Lippincott-Schwartz, 2002; Sinnecker et al., 2005). The stochastic recovery of the fluorophores from this “dark” state is used for optical isolation of the single molecule signals. Like in other techniques of localisation microscopy, this allows a precise position determination (down to a few nanometres) of the detected fluorophores.

So far, all localisation microscopy approaches used fluorochrome labelled molecules and fluorescent proteins, respectively. Very recently a method has been described to image fluorophores with undetectable fluorescence by stimulated emission microscopy (Min et al., 2009). This technique allowed various applications to analyse the cellular distribution of so far undetectable molecules; the optical resolution, however, corresponded to the conventional one. In the present report we show that SPDM has the capability of imaging label-free cellular structures,

* Corresponding author at: Applied Optics and Information Processing, University Heidelberg, Im Neuenheimer Feld 227, D-69120 Heidelberg, Germany.
Tel.: +49 6221 54 9252; fax: +49 6221 54 9112.

E-mail address: cremer@kip.uni-heidelberg.de (C. Cremer).

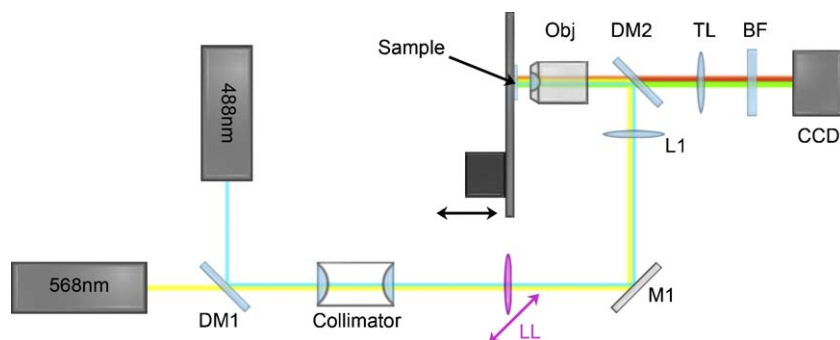


Fig. 1. SPDM setup. The setup used for the experiments presented in this report is shown schematically in the above figure. Excitation and detection pathway are similar to a conventional wide-field fluorescence microscopy setup, except for the lens [LL]. It allows the adjustment of the illumination intensity in the object space to achieve the appropriate conditions for SPDM.

including structures with so far undetectable fluorescence with localisation accuracies in the 20 nm range.

2. Materials and methods

2.1. SPDM setup

Measurements were accomplished by using the SPDM setup (Gunkel et al., 2009; Kaufmann et al., 2009; Lemmer et al., 2008, 2009). The light induced reversibly bleached state of the molecules, that is necessary for optical isolation, is achieved by illumination with a laser intensity of 10 kW/cm² to several 100 kW/cm². In this manner some fluorophores are either switched to a reversibly bleached state ($M_{fl} \rightarrow M_{rbl}$) or to an irreversibly bleached state ($M_{fl} \rightarrow M_{ibl}$). The stochastic recovery of the molecules from the reversibly bleached state ($M_{fl} \leftarrow M_{rbl}$) is used for optical isolation of the detected molecules. This method enables localisation microscopy with conventionally labelled cells and even completely label-free cells, as it is presented in this report.

The microscopy setup provides two DPSS laser sources with a wavelength of 488 nm (Sapphire HP 488, Coherent, Dieburg, Germany) and 568 nm (Sapphire 568, Coherent, Dieburg, Germany). The laser beams are combined and expanded by a factor of 2.5 before being focused into the back focal plane of an oil immersion objective lens (HCX PL APO, 63x, NA = 0.7–1.4, Leica, Wetzlar, Germany). Fluorescent light emitted by the sample passes through a dichroic mirror (AHF Analysentechnik, Tübingen, Germany) and a blocking filter (AHF Analysentechnik, Tübingen, Germany) before being focused onto the CCD chip of a sensitive camera (SensiCam QE, PCO Imaging, Kehlheim, Germany). An additional lens is mounted in the excitation pathway to increase the laser intensity in the object plane for obtaining appropriate conditions for the reversibly photo bleaching (Fig. 1).

2.2. Data acquisition and evaluation

Data stacks consisting of several thousand images were recorded with an integration time of the camera between 10 and 50 ms. The first step of the data evaluation is a conversion of the count numbers in the acquired images into the corresponding photon numbers. Due to high background noise and bleaching gradients in biological samples the signals of single molecules have to be filtered out by calculating a differential image stack. This is done by subtracting the succeeding from the preceding frame. After segmentation of the raw data, a model function (2D Gaussian) was fitted to the single molecule signals for determination of their lateral positions (for more detail see Kaufmann et al., 2009; Lemmer et al., 2008, 2009). The gathered information is used to render a localisation image. Therefore all positions of the detected molecules were

merged into one image and blurred with a Gaussian corresponding to their individual localisation accuracy. The effective optical resolution of this image is given by the density of detected signals and the localisation accuracy.

2.3. Specimen preparation

Cal-51 (German Resource Centre for Biological Material—DSMZ, Braunschweig, Germany) and SKBr3 (American Type Culture Collection—ATCC, Manassas, USA) are two mamma carcinoma cell lines from pleural effusion. Cal-51 were cultivated in DMEM medium supplemented with 20% FCS, 1% L-glutamine, 1% penicillin/streptomycin and SKBr3 in McCoy's 5a medium with 10% FCS, 1% L-glutamine, 1% penicillin/streptomycin in a standard CO₂-incubator. The cells were seeded onto cover slips (24 mm × 24 mm) and allowed to attach and to grow overnight. Cells were fixed with 4% formaldehyde in PBS and embedded with ProLong[®] Gold antifade reagent (Invitrogen, Carlsbad, USA). Imaging of these label-free specimens was performed by the previously described SPDM setup.

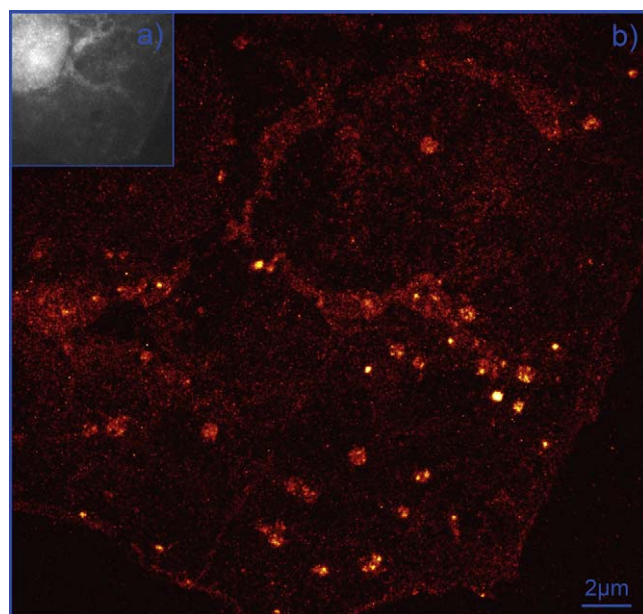


Fig. 2. Localisation image of label-free Cal-51 cell. (a) Conventional wide-field fluorescence image of a Cal-51 cell before the SPDM measurement. Structural details are visible due to autofluorescence. (b) The same region of the cell using SPDM for image acquisition. In both images membrane structures are visible. The very bright spherical objects with diameters in the 1 μm range are only visible in the localisation image. Excitation was done using a laser with a wavelength of 488 nm.

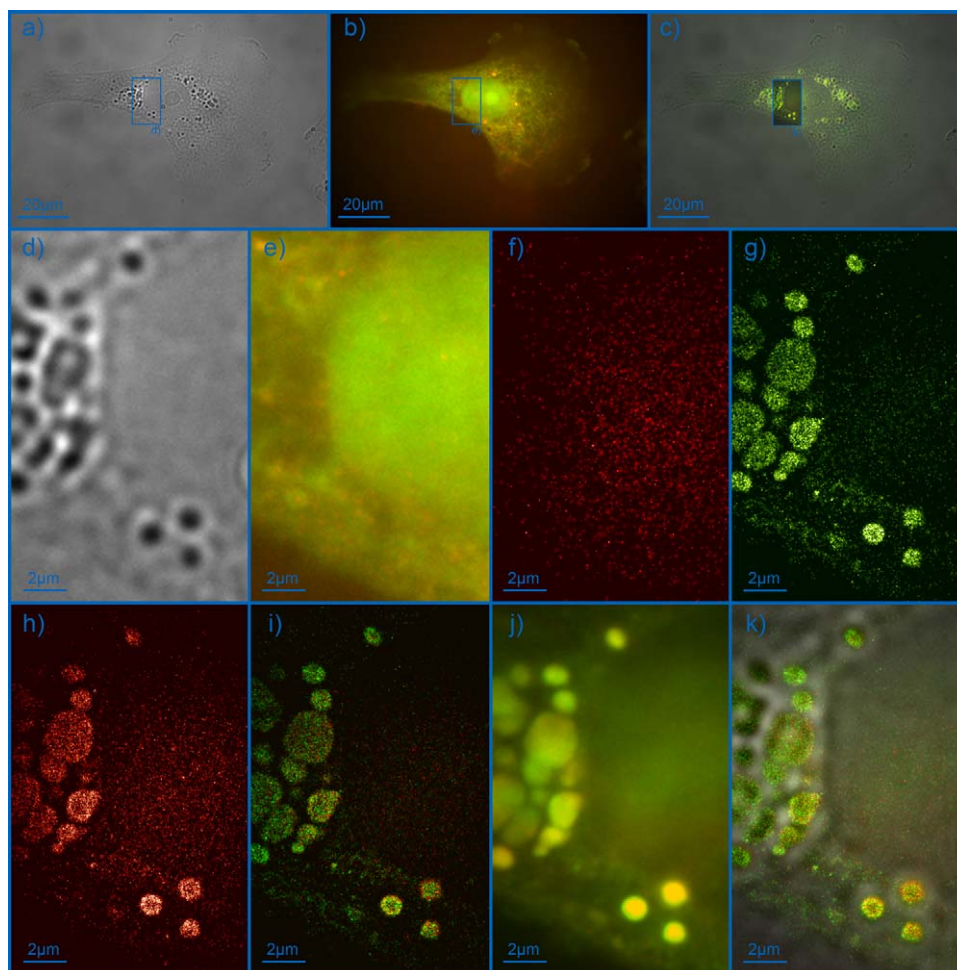


Fig. 3. Label-free SKBr3 cell excited with 488 and 568 nm. (a) Bright-field image of a SKBr3 cell. Several dark spots are clearly recognizable in the cytoplasm. (b) Conventional wide-field fluorescence image of the same cell taken before the SPDM measurements. The red channel shows excitation with 568 nm, the green channel excitation with 488 nm. The objects, which are visible as dark spots in the bright-field image are missing in the fluorescence image (compare (d) and (e)). (f) Localisation image acquired with an excitation at 568 nm. No structural details are visible. Afterwards a second localisation image (g) was acquired using illumination with 488 nm. Spherical objects are clearly recognizable at the positions where the dark spots were detected in the bright-field image. (h) Result of a SPDM measurement with an excitation wavelength of 568 nm after fluorescence activation of molecules by the 488 nm laser used in the previous measurement (g). This localisation image revealed the same spherical objects as the one with 488 nm excitation (see merged image in (i)). These objects also became visible in a conventional wide-field image taken after the SPDM measurements (j). (c and k) Merged images of the bright-field image, the wide-field fluorescence image acquired after the SPDM measurements and the two secondary localisation images.

3. Results

SPDM measurements of human breast cancer cells Cal-51 and SKBr3 show that it is possible to obtain localisation images of cellular structures without any labelling. Both conventional wide-field fluorescence and SPDM measurements revealed membrane structures due to autofluorescence of the cells. In the localisation images (Figs. 2b, 3g–i and 5b and d), spherical objects with a size in the μm range are clearly visible, which cannot be observed in the conventional wide-field fluorescence images. However, bright-field images show these cellular spherical objects localised in the cytoplasm as dark spots (compare Fig. 3a, b, d and e) SPDM measurements using a yellow laser with a wavelength of 568 nm do not yield any structural details (Fig. 3f), whereas SPDM measurements with an excitation of 488 nm obviously do (Fig. 3g). The positions of the spherical objects in the localisation image match these in the bright-field image.

To investigate the fluorescence dynamics of the detected molecules, a secondary SPDM measurements of the same region as before has been performed at an excitation wavelength of 568 nm (Fig. 3h). This was done directly after the SPDM measurement with 488 nm. Only now it became possible for the excitation with 568 nm

to detect the same structures as in the measurement using the 488 nm laser (Fig. 3i). The spherical objects are also visible in the wide-field fluorescence images acquired after the SPDM measurements (Fig. 3j). These results indicate a fluorescence activation of particular molecules in the cell. SPDM measurements with an excitation wavelength of 568 nm reveal structural details of the cell, only if an activation with appropriate wavelength and illumination intensity (for presented data: 488 nm at 50–100 kW/cm^2) was applied before or during data acquisition.

Regarding the number of detected molecules over time (100 s) for the SPDM measurements of a SKBr3 cell with 568 nm after activation and 488 nm, a very different behaviour has been observed (Fig. 4). Excitation with 488 nm resulted in an increasing number of detected signals during data acquisition (Fig. 4a). This again indicates fluorescence activation of the molecules in the sample, which are recorded during the SPDM measurement. In contrast to this result, a decreasing number of detected signals have been observed for the SPDM measurement at 568 nm after activation (Fig. 4b). The same characteristic features of the data shown in this histogram are expected for conventional fluorophores, being bleached during the measurement without fluorescence activation.

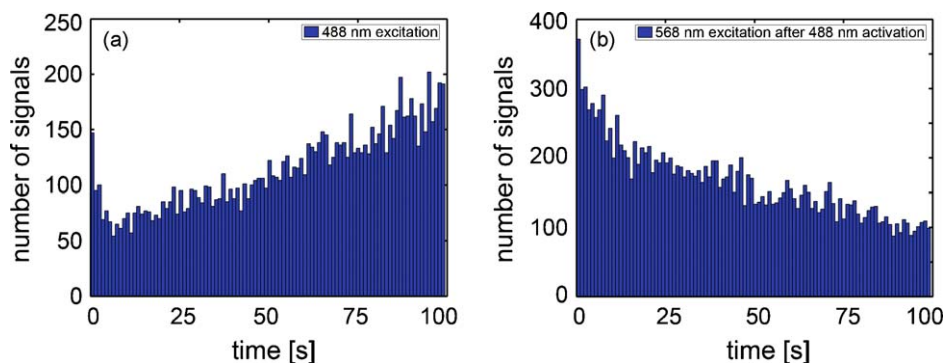


Fig. 4. Histograms of detected signals over time for 488 and 568 nm SPDM measurements. In both histograms the number of detected signals over time is depicted. The width of the bars corresponds to a time interval of 1 s (20 frames). (a) Increase of signals over time during a SPDM measurement with excitation of 488 nm (see Fig. 3g). This indicates a fluorescence activation of molecules in the cell. (b) Result of a SPDM measurement with 568 nm excitation, done afterwards (see Fig. 3h). Here, a decrease of detected signals over time is recognisable.

In Fig. 5 a more detailed characterisation of the structures visible in the localisation images of a label-free SKBr3 cell is depicted. The spherical structures display a remarkably high density of detected signals (several $1000/\mu\text{m}^2$). For two of these objects (highlighted in orange) the mean density was determined (Fig. 5b), which shows a density for the smaller one of $8728\text{ signals}/\mu\text{m}^2$, whereas the larger object consists of $6007\text{ signals}/\mu\text{m}^2$. The membrane structures, visible in both wide-field and localisation images, reveal an obviously lower density of detected signals. Therefore, the dynamic range of the localisation image has to be changed accordingly to visualise these thin structures besides the extremely “bright” spherical objects (Fig. 5d). A line-scan (drawn in yellow) with a line width of 200 nm was applied to one of the spherical objects in the conventional wide-field image after fluorescence activation (Fig. 5a) and the corresponding localisation image (Fig. 5b). A comparison of the line-scans is shown in Fig. 5c. Both line-scans illustrate clearly that more of the detected molecules are located on the periphery, rather

than in the centre of the object. The shape can be determined more precisely using the localisation data due to a higher effective optical resolution in the 60 nm range for this area. Because of the lack of out of focus signals in localisation microscopy images also the contrast is enhanced compared to a conventional wide-field fluorescence image.

4. Discussion

In the last years, sub-diffraction limit light microscopy techniques of fluorescent labelled cellular structures have been firmly established. In particular, various approaches of localisation microscopy allowed the localisation single molecules with an accuracy down to the few nanometre regime.

So far no reports have been available where localisation microscopy of label-free cellular structures has been performed. In contrast to a recently published report, using stimulated emission

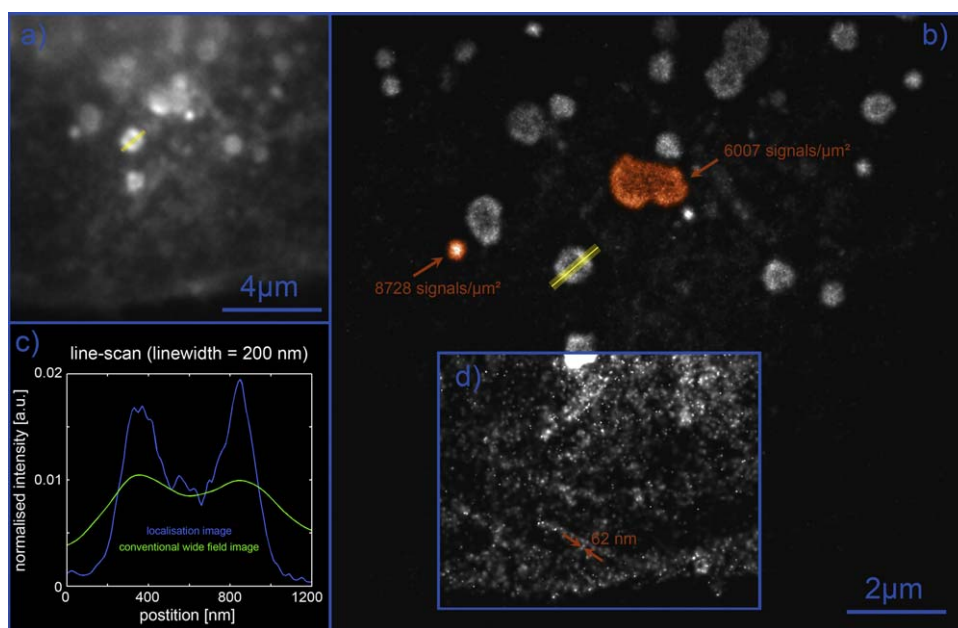


Fig. 5. Characterisation of structures in localisation image of a label-free SKBr3 cell. (a) Wide-field image of an area of a label-free SKBr3 cell taken after a SPDM measurement with an excitation wavelength of 488 nm. (b) Result of the SPDM measurement. The mean localisation accuracy of the about 100,000 detected signals was 31.5 nm with a standard deviation of 10.7 nm. A line-scan (drawn in yellow) with a line width of 200 nm was applied to one of the spherical objects. (c) Comparison between the line-scan in the wide-field image and the localisation image. Both curves are normalised to their integral. For highlighting thin structures in the localisation image the dynamic range of an area (d) was changed accordingly. The spherical structures are strongly oversaturated in this rendering due to the high density of detected signals (several $1000/\mu\text{m}^2$) for these objects.

as a diffraction limited light optical method for visualizing undetectable cellular fluorophores (Min et al., 2009), SPDM is capable to obtain sub-diffraction limit images of structures in label-free cells. Localisation accuracy and the density of detected signals result in an effective optical resolution down to the 20 nm range. Due to single molecule information provided in localisation microscopy, it might be possible to analyse these cellular structures in a quantitative way, if the responsible fluorescent molecules could be verified and characterised by methods of molecular biology and photo chemistry/physics.

Our experiments had shown that besides membrane structures, which are also detectable in conventional wide-field fluorescence images, spherical objects could be visualised by SPDM in label-free cells. Our observations with excitation at different wavelengths (Fig. 3) as well as the signal amplitude vs. time (Fig. 4) evoke the assumption of a fluorescence activation of the detected molecules. It allows suppressing or enhancing the observed fluorescence dynamics of particular cellular molecules by appropriate choice of illumination.

The fluorescence activation may be some photo conversion of the molecule itself or a conversion of a neighbouring molecule quenching its fluorescence (e.g. most of the flavins existing as enzyme cofactors (Kunz and Kunz, 1985; Voltti and Hassinen, 1978). Most of the cellular autofluorescence arises from proteins containing aromatic aminoacids, the reduced form of pyridine nucleotides (NAD(P)H), flavins and lipopigments (Benson et al., 1979; Dayan and Wolman, 1993; Galeotti et al., 1970; Udenfried, 1969). The majority is originated in mitochondria and lysosomes and their excitation maxima are mostly in the blue and UV range of the electromagnetic spectrum (Monici, 2005). We tried to determine the observed spherical structures by immunofluorescence labelling of lysosomes (LAMP1 and LAMP2, Santa Cruz Biotechnology, Heidelberg, Germany) and early endosomes (Anti-EEA1, BD Transduction Laboratories, New Jersey, USA). Our results (data not shown) yielded no coincidence of these markers with the observed spherical objects. Further analysis has to be done for a clear identification of these cellular vesicles.

Numerous applications have been reported using the fluorescence of granules accumulated in the cytoplasm as a diagnostic technique (e.g. ageing (Shimasaki et al., 1980; Tsuchida et al., 1987), cancer (Matsumoto, 2001; Shin et al., 2000), and retinal degeneration (Stark et al., 1984)). Due to sub-diffraction limit resolution and single molecule information provided in SPDM, label-free cellular structures could be analysed in a precise and quantitative way and thus also be used as a diagnostic tool in future applications.

To summarize, the study presented here shows that sub-diffraction limit light microscopy using a localisation microscopy method (SPDM) can be applied not only to fluorescence labelled cells but even also to label-free cellular structures.

Acknowledgements

The financial support of the University Heidelberg (Frontier Project grant to M. Wassenegger); of the Deutsche Forschungsgemeinschaft (SPP1128); and of the European Union (In Vivo Molecular Imaging Consortium, www.molimg.gr) to Christoph Cremer is gratefully acknowledged. Patrick Müller is supported by a grant of the Federal Ministry of Education and Research (BMBF) to Michael Hausmann (Services@MediGRID).

We also thank our colleagues Dr. Paul Lemmer, Manuel Gunkel, Yanina Weiland, Heinz Eipel, Margund Bach and Dr. Sascha Keller (DKFZ) for great support.

References

- Abbe, E., 1873. Beitrage zur Theorie des Mikroskops und der mikroskopischen Wahrnehmung. *Archiv f. mikroskopische Anatomie* 9, 411–468.
- Benson, R.C., Meyer, R.A., Zaruba, M.E., McKhann, G.M., 1979. Cellular autofluorescence—is it due to flavins? *J. Histochem. Cytochem.* 27, 44–48.
- Betzig, E., Patterson, G.H., Sougrat, R., Lindwasser, O.W., Olenych, S., Bonifacio, J.S., Davidson, M.W., Lippincott-Schwartz, J., Hess, H.F., 2006. Imaging intracellular fluorescent proteins at nanometer resolution. *Science* 313, 1642–1645.
- Dayan, D., Wolman, M., 1993. Lipids pigments. *Prog. Histochem. Cytochem.* 25, 1–75.
- Esa, A., Edelmann, P., Trakthenbrot, L., Amariglio, N., Rechavi, G., Hausmann, M., Cremer, C., 2000. Three-dimensional spectral precision distance microscopy of chromatin nanostructures after triple-colour DNA labelling: a study of the BCR region on chromosome 22 and the Philadelphia chromosome. *J. Microsc.* 199 (2), 96–105.
- Galeotti, T., Van Rossum, G.D.V., Mayer, D.H., Chance, B., 1970. On the fluorescence of NAD(P)H in whole cell preparations of tumors and normal tissues. *Eur. J. Biochem.* 17, 485–596.
- Gunkel, M., Erdel, F., Rippe, K., Lemmer, P., Kaufmann, R., Hörmann, C., Amberger, R., Cremer, C., 2009. Dual color localization microscopy of cellular nanostructures. *Biotechnol. J.* 4, 927–938.
- Hendrix, J., Flors, C., Dedeker, P., Hofkens, J., Engelborghs, Y., 2008. Dark states in monomeric red fluorescent proteins studied by fluorescence correlation and single molecule spectroscopy. *Biophys. J.* 94, 4103–4113.
- Hess, S.T., Girirajan, T.P.K., Mason, M.D., 2006. Ultra-high resolution imaging by uorescence photoactivation localization microscopy. *Biophys. J.* 91, 4258–4272.
- Kaufmann, R., Lemmer, P., Gunkel, M., Weiland, Y., Müller, P., Hausmann, M., Baddeley, D., Amberger, R., Cremer, C., 2009. SPDM—single molecule superresolution of cellular nanostructures. *Proc. SPIE* 7185, 1–19 (invited paper).
- Kunz, W.S., Kunz, W., 1985. Contribution of different enzymes to flavoprotein fluorescence of isolated rat liver mitochondria. *Biochim. Biophys. Acta* 841, 237–246.
- Lemmer, P., Gunkel, M., Baddeley, D., Kaufmann, R., Urich, A., Weiland, Y., Reymann, J., Müller, P., Hausmann, M., Cremer, C., 2008. SPDM: light microscopy with single-molecule resolution at the nanoscale. *Appl. Phys. B* 93 (1), 1–12.
- Lemmer, P., Gunkel, M., Baddeley, D., Kaufmann, R., Weiland, Y., Müller, P., Urich, A., Amberger, R., Eipel, H., Hausmann, M., Cremer, C., 2009. Using conventional fluorescent markers for far-field fluorescence localization nanoscopy allows resolution in the 10 nm regime. *J. Microsc.* 235, 163–171.
- Matsumoto, Y., 2001. Lipofuscin pigmentation in pleomorphic adenoma of the plate. *Oral Surg. Oral Med. Oral Pathol.* 3, 299–302.
- Min, W., Lu, S., Chong, S., Roy, R., Holtom, G.R., Xie, S., 2009. Imaging chromophores with undetectable fluorescence by stimulated emission microscopy. *Nature* 461, 1105–1109.
- Monici, M., 2005. Cell and tissue autofluorescence research and diagnostic applications. *Biotechnol. Annu. Rev.* 11, 227–256.
- Patterson, G.H., Lippincott-Schwartz, J., 2002. A photoactivatable GFP for selective photolabeling of proteins and cells. *Science* 297, 1873–1877.
- Rayleigh, L., 1896. On the theory of optical images, with special reference to the microscope. *Philos. Mag.* 42 (5), 167–195.
- Rauch, J., Knoch, T.A., Solovei, I., Teller, K., Stein, S., Buiting, K., Horsthemke, B., Langowski, J., Cremer, T., Hausmann, M., Cremer, C., 2008. Lightoptical precision measurements of the active and inactive Prader–Willi syndrome imprinted regions in human cell nuclei. *Differentiation* 76, 66–82.
- Rust, M.J., Bates, M., Zhuang, X., 2006. Sub-diffraction-limit imaging by stochastic optical reconstruction microscopy (STORM). *Nat. Methods* 3, 793–795.
- Shimasaki, H., Ueta, N., Privett, O.S., 1980. Isolation and analysis of age-related fluorescent substances in rat testes. *Lipids* 15, 236–241.
- Shin, S.J., Kanomatra, N., Rosen, P.P., 2000. Mammary carcinoma with prominent cytoplasmic lipofuscin granules mimicking melanocytic differentiation. *Histopathology* 37, 456–459.
- Sincker, D., Voigt, P., Hellwig, N., Schaefer, M., 2005. Reversible photobleaching of enhanced green fluorescent proteins. *Biochemistry* 44, 7085–7094.
- Stark, W.S., Miller, G.V., Itoku, K.A., 1984. Calibration of microspectrophotometers as it applies to the detection of lipofuscin and blue- and yellow-emitting fluorophores in situ. *Methods Enzymol.* 105, 341–347.
- Tsuchida, M., Miura, T., Aibara, K., 1987. Lipofuscin and lipofuscin-like substances. *Chem. Phys. Lipids* 44, 297–325.
- Udenfried, S., 1969. *Fluorescence Assay in Biology and Medicine*, vol. 2. Academic Press, New York/London, pp. 491–492.
- Voltti, H., Hassinen, I.E., 1978. Oxidation-reduced midpoint potentials of mitochondria flavoproteins and their intramitochondrial localization. *J. Bioenerg. Biomembr.* 10, 45–58.